JLR RESEARCH ARTICLE

Elevation of hepatic de novo lipogenesis in mice with overnutrition is dependent on multiple substrates

Jordan W. Strober[1], Stephan Siebel[2], Susan F. Murray[3], Manuel González Rodríguez[4], Carlos Rodriguez-navas Gonzalez[5], and Daniel F. Vatner[1,5,6,*]

[1]Department of Internal Medicine, Yale School of Medicine, New Haven, CT; [2]Department of Pediatrics, Yale School of Medicine, New Haven, CT; [3]Ionis Pharmaceuticals, Inc., Carlsbad, CA; [4]Department of Neurology, Icahn School of Medicine at Mount Sinai, New York, NY; [5]Department of Medicine, Veterans Affairs Medical Center, New Haven, CT; and [6]Program in Translational Biomedicine, Yale School of Medicine, New Haven, CT

Abstract **Increased de novo lipogenesis (DNL) contributes to hyperlipidemia, MASLD, and ASCVD in insulin-resistant subjects. However, multiple pathways support lipogenesis and few have sought to quantify the contributions of the discrete metabolic pathways that contribute to lipogenesis. In this study, antisense oligonucleotides (ASOs) targeting glucokinase (*Gck*), lactate dehydrogenase A (*Ldha*), and glutamic-pyruvic transaminase 2 (*Gpt2*) were utilized to restrict substrate flux from lipogenic precursors in C57BL6/J mice, comparing controls (CO) and chronic overnutrition (ON). In CO mice, ASO treatments did not significantly alter lipogenesis; however, there was a trend toward decreased hepatic triglyceride content and DNL, especially with the GPT2 ASO (TG = −46.8%; DNL = −53.7%). Expectedly, increased hepatic TG content and DNL (ON vs. CO: TG = +187.9%; DNL = +41.8%) were observed in mice with chronic overnutrition. Gas chromatography-mass spectrometry analyses demonstrated increased hepatic TCA cycle metabolites (ON vs. CO: fumarate +74.2%; malate +54.0%; and citrate +43.2) and decreased hepatic concentrations of multiple amino acids (ON vs. CO: Leu −41.7%; Ile −45.0%; Val −56.3%; Ser −22.6%). With ON, TG content and DNL were reduced by restricting lipogenic carbon entry from alanine (GPT2: TG = −45.5%; DNL = −48.1%), lactate (LDHA: TG = −25.8%; DNL = −33.1%), or glucose (GCK: TG = −59.2%; DNL = −69.2%). Amino acids appear to be a consistent carbon source for DNL in mice; however, carbon entry from all sources is required to maintain the significantly elevated rates of hepatic DNL in chronically overfed mice. These findings may inform the development of novel therapies and underscore the importance of peripheral substrate storage and oxidation in the prevention of dyslipidemia in the metabolic syndrome.**

Supplementary key words triglyceride • liver • insulin resistance • lipolysis and fatty acid metabolism • mitochondria • de novo lipogenesis • antisense oligonucleotide • TCA cycle

Disordered lipid metabolism is a hallmark of insulin resistance and Type 2 Diabetes (T2D). Insulin-resistant patients experience high rates of metabolic dysfunction-associated steatotic liver disease (MASLD), the most common chronic liver disease, and atherosclerotic cardiovascular disease (ASCVD), the leading cause of morbidity and mortality for diabetic patients) (1–3). Increased hepatic de novo lipogenesis (DNL) is a central feature of dysregulated lipid metabolism (4–6). While carbon flux to the liver is well known to be altered in insulin-resistant animals, the discrete pathways that contribute to increased DNL in insulin-resistant animals are yet to be determined.

Nutrients influence hepatic DNL through multiple mechanisms. They can act as substrates, providing an influx of carbon into citrate, or can act to regulate the transcription regulation of lipogenesis; either directly, or through hormonal regulation. Insulin action, in response to glucose, stimulates DNL via sterol regulatory element binding protein-1c (SREBP-1c), which activates the transcription of genes encoding enzymes required for lipid synthesis (7–9). However, changes in substrate flux may play a critical role in supporting the increase in DNL observed in the setting of insulin resistance (10–12). One mechanism by which substrate, specifically glucose or fructose, can directly regulate DNL is via activation of the lipogenic transcription factor carbohydrate response element binding protein (ChREBP) (13, 14). This process is adept at activating lipogenic machinery to promote energy storage in response to a high-carbohydrate meal, but chronic overconsumption of sugar induces hepatic lipid deposition, contributing to the development of metabolic dysfunction-associated steatotic liver disease (MASLD) (15). Beyond the transcriptional regulation of lipid metabolism afforded by insulin-driven SREBP-1c and carbohydrate-driven ChREBP, multiple

*For correspondence: Daniel F. Vatner, daniel.vatner@yale.edu.

ASBMB

Published by Elsevier Inc on behalf of American Society for Biochemistry and Molecular Biology.

https://doi.org/10.1016/j.jlr.2025.100838

substrate fluxes are thought to contribute to DNL via substrate push (12, 16, 17). Multiple substrates, including lactate, amino acids, glucose, and fructose, provide carbon for mitochondrial pyruvate and drive hepatic DNL (18). Furthermore, in insulin-resistant subjects, a surplus of these substrates (19) is associated with an increase in DNL and can drive the development of MASLD (20). Although it is established that metabolic fluxes are perturbed in the insulin-resistant subject, the role of specific substrate contributors to hepatic DNL has not been sufficiently studied to answer this critical question. If increased DNL in the insulin-resistant liver is not solely due to altered transcription of lipogenic regulators, it may also be due to one or more carbon fluxes that support the production of mitochondrial pyruvate leading to increased DNL via citrate synthesis.

In the present study, we sought to elucidate the contribution of different substrates that support mitochondrial pyruvate metabolism and hepatic DNL during hepatic insulin resistance, which is well described to develop with chronic overnutrition (21, 22). To address this question, antisense oligonucleotides (ASOs) targeting glucokinase (*Gck*), lactate dehydrogenase (*Ldha*), and glutamic-pyruvic transaminase 2 (*Gpt2*) were applied to restrict substrate influx from specific lipogenic precursors in both control and chronic overnutrition chronic overnutrition C57BL6/J mice. This will provide a deeper understanding of the roles of individual pyruvate-producing substrates when DNL is increased in the setting of insulin resistance and should inform future studies of novel therapies for the treatment of lipid dysmetabolism in insulin-resistant patients.

MATERIALS AND METHODS

Animals

C57BL/6 mice (9 weeks old) were obtained from Jackson Laboratory (Bar Harbor, ME, USA). Animals were housed under controlled temperature (23°C) and lighting (12 h light/dark cycle, lights on at 07:00) with free access to water and food. Mice were maintained on standard regular chow (Envigo 2108S: 24% protein, 58% carbohydrate, 18% fat; Envigo, Madison WI, USA) and were placed on a high-fat diet (HFD) (Research Diets D12492: 20% protein, 20% carbohydrate, 60% fat; Research Diets, Inc., New Brunswick, NJ, USA) for the study.

One cohort of mice was fed an HFD for 6 weeks to induce whole-body lipid-induced insulin resistance, which is described to develop in mice in a tissue-specific manner with chronic overnutrition (21, 22). Another age-matched control cohort was only fed the HFD for the final three days of the study to provide a relatively insulin-sensitive group that is matched in terms of dietary substrate composition (23). All mice, from both the control (CO) and the chronic overnutrition (ON) cohorts, were provided 1% dextrose drinking water for the final three days of the study to amplify the rates of de novo lipogenesis that were blunted by the high-fat feeding.

Antisense oligonucleotides (ASOs) were administered twice by intraperitoneal injection, one week apart, beginning 10 days before the end of the study. A 2′-O-methoxyethyl (MOE) glucokinase (*Gck*) ASO was compared with an MOE control ASO, while N-acetylgalactosamine (GalNAc) lactate dehydrogenase A (*Ldha*) and glutamic pyruvate transaminase 2 (*Gpt2*) ASOs were compared with a GalNAc control ASOs (control ASOs do not target any known gene). The MOE ASO dose was 75 mg/Kg-wk, while the GalNAc ASO dose was 15 mg/kg-wk.

All procedures were approved by the Institutional Animal Care and Use Committee of the Yale University School of Medicine. For the studies, mice were given ad libitum access to food overnight and placed in restrainers (without food) upon initiation of the light cycle (7am). Animals were euthanized 3–4 h later under isoflurane anesthesia. Care was taken throughout the study to minimize suffering.

In vivo de novo lipogenesis

Three days before sacrifice, total body water deuterium enrichment was increased by a 23.4 ml/kg subcutaneous injection of 99% ^{2}H-enriched saline (Cambridge Isotope Laboratories). The mice were given 6% (vol/vol) $^{2}H_2O$-enriched drinking water for the ensuing three days. Liver and plasma were taken during euthanasia under isoflurane.

Triglyceride palmitate deuterium enrichment was determined by GC-MS and de novo hepatic palmitate synthesis was calculated from isotopic data as previously described (11, 24–26). Hepatic lipid samples (in chloroform) were spotted onto Silica gel 60 plates, and TLC was performed with a mobile phase of hexane:diethyl ether:acetic acid (80:20:1). Plates were developed with 0.005% primuline in acetone:water (80:20). Purified samples were collected while absorbed to Silica and eluted with diethyl ester. Triglyceride-fatty acids were analyzed by GC-MS (5975CI, Agilent Technologies) as fatty acid methyl esters following derivatization with methanolic boron trifluoride. The plasma $^{2}H_2O$ pool was assessed by the exchange of hydrogens from plasma to acetone in the presence of sodium hydroxide; acetone deuterium enrichment was analyzed by GC-MS.

U^{13} C glutamine tracer analysis

Uniformly labeled glutamine was infused in fed mice to determine relative differences in label distribution within the TCA induced by diet and ASO treatment. In preparation for glutamine infusion, Instech catheters (Part Number: C20PU) were placed in the jugular vein 7 days before the infusions. Only mice that recovered more than 95% of their preoperative body weight were studied. Mice were provided ad libitum access to food overnight and all studies began at 08:00 the following morning. For infusions, awake mice under gentle tail restraint underwent a primed-continuous infusion of [13C5]glutamine (Cambridge Isotope Laboratories) at 18.0 μmol/(kg-min) for 5 min. Infusion rates were then lowered to 6.0 μmol/(kg-min) and the infusion continued for 115 min. Blood samples were collected by tail bleeding at 120′ for determination of plasma glucose and insulin. All mice were anesthetized with intravenous pentobarbital sodium injection (150 mg/kg), and tissues were rapidly harvested and snap-frozen with clamps precooled in liquid nitrogen. Tissues were stored at −80°C for subsequent analysis.

Isotope enrichment and metabolic flux were assessed as previously described (27). Briefly, metabolite concentrations and 13C-enrichments were determined by mass spectrometry using a 6500+ QQQ SelexION. Samples (4 µl) were injected onto a Hypercarb column (3 µm particle size, 3 × 150 mm, Thermo Fisher Scientific) at a flow rate of 1 ml/min. Metabolites were eluted with a combination of aqueous (A: 2.0 mM ammonium acetate and 12.5 mM triethylamine) and organic mobile phase (B: 95% acetonitrile, 5% water 2.0 mM ammonium acetate and 12.5 mM triethylamine) according to the following gradient: t = 0 min, B = 0%; t = 0.5 min, B = 0%, t = 5 min, B = 15%; t = 5.25 min, B = 50%; t = 6.25 min, B = 50%; t = 6.5 min, B = 0%; t = 8 min, B = 0%. Metabolite detection was based on multiple reaction monitoring (MRM) in negative mode using the source parameters in Supplemental Table 1. Separation Voltage (SV) and Compensation Voltage (CoV) were optimized individually for each metabolite in order to maximize signal intensity and isobar resolution. The individual MRM transition pairs (Q1/Q3) are listed in Supplemental Table 2. Retention times were confirmed with known standards and peaks integrated using El-Maven (Elucidata). The atomic percent excess (APE) was calculated using the Polly interface (Elucidata) and corrected for background noise and natural abundance. The sum of all measured metabolites in each sample was used as an internal control. Metabolite concentrations were normalized to protein content determined by standard Bradford protein assay.

Hepatic triglyceride content

Hepatic triglycerides were extracted as previously described (10). Briefly, lipids were extracted with 2:1 chloroform: methanol and triglyceride content were measured (Sekisui Triglyceride-SL kit; Sekisui Diagnostics).

Plasma biochemical analysis

Glucose concentrations were determined using a YSI 2700 select (Yellow Springs Instruments, Yellow Springs, OH, USA) or a standard spectrophotometric assay (Sekisui). Kits were also used to measure nonesterified fatty acids (NEFAs; Wako) and triglyceride (Sekisui). Insulin was measured by radioimmunoassay (EMD Millipore). Serum ALT (Abcam, ab105134) and AST (Cayman Chemical, 701,640) were both measured by colorimetric assay.

Hepatic biochemical analysis

Colorimetric assays were used to measure both hepatic β-hydroxybutyrate (Cayman Chemical, 700,190) and acetoacetate (Abcam, ab180875).

Immunoblotting

Proteins from tissue lysate were resolved by SDS-PAGE using a 4%–12% gradient gel and electroblotted onto polyvinylidene difluoride membranes (EMD Millipore). Membranes were blocked with 3% BSA in TBST and incubated in primary antibodies overnight. After washing, horseradish peroxidase-conjugated secondary antibodies (Cell Signaling Technology; 1:5000) were applied for one hour and detection was performed with enhanced chemiluminescence.

Primary antibodies used included β-Actin (Sigma, AC-15; 1:5000), GCK (Santa Cruz, 7908; 1:500), GPT2 (Proteintech, 16757-1-AP; 1:1000), and LDHA (Cell Signaling, 2012S; 1:5000).

Quantitative real-time polymerase chain reaction

Following tissue homogenization, RNA was extracted using the RNeasy® Mini Kit (Qiagen, 74,106). Following RNA extraction, QuantiTect Reverse Transcription Kit was used to produce cDNA (Qiagen, 205,311). Gene expression for genes of interest was measured with quantitative real-time polymerase chain reaction (qRT-PCR). The gene beta actin (*Actb*) was used as an internal reference throughout all measured genes. Primer sequences for the referenced genes are listed (Table 1).

Metabolomics

TCA cycle, glycolysis, and amino acid intermediates were analyzed using gas chromatography-mass spectrometry in an Agilent 5977B GC/MSD as previously described (28). Briefly, 20 mg of frozen liver were homogenized in a Next Advance Bullet Blender, using 1 ml of cold water/methanol/acetonitrile (1:2:2). After centrifugation, supernatant solvents were transferred into a GC vial and then dried with N2 gas. The extracts were reconstituted with 20ul of MSTFA +1% TBDMCS (N-Methyl-N-(trimethylsilyl)trifluoroacetamide) and 40ul of acetonitrile, and heated 45 min at 75C to generate TMS derivatives, following the injection of 1 µl of the sample into the GCMS. TMS derivatives were identified by their retention time and unique mass features using Electron Ionisation SIM. Compounds were quantified utilizing Internal Standard calibration curves and Tricarballylic acid was added as a surrogate. All metabolomics data, including undiscussed data, is provided in the supplement.

Statistical analysis

Statistical analysis was performed using GraphPad Prism 10 (GraphPad Software). For direct comparisons between the two groups, the Student's unpaired *t* test was utilized. When comparing multiple groups, a one-way ANOVA was used with various post hoc analyses depending on the setting. If only one control was being utilized in a comparison Dunnett's multiple comparison test was performed; however, in a comparison with multiple controls Šídák's multiple comparisons test was used. In cases with direct comparisons to separate controls, where the one-way ANOVA was significant, Fisher's LSD test was conducted. All data are expressed as mean ± SEM. *P* values less than 0.05 were considered significant.

RESULTS

Effect of ASO treatment in 3-day high-fat fed mice is small

The impact of substrate restriction on DNL was first assessed CO mice fed a high-fat diet and 1% dextrose drinking water during the three days of DNL assessment. Mice were administered ASO's against *Gck*, *Ldha*, and *Gpt2* – reducing the hepatic gene expression and protein abundance of the targeted enzymes (**Fig. 1**). ASO treatments did not cause transaminitis, induce weight loss, or create any significant changes to tail-vein blood glucose or insulin levels (Table 2).

In the CO mice the effect of ASO treatment was small and not significant; however, each ASO induced a decrease in both hepatic lipogenesis (GCK: 33%, $P < 0.2$;

TABLE 1. Primer list. Primer sequences are provided for all genes tested by qPCR

Gene	Forward Sequence (5′-3′)	Reverse Sequence (5′-3′)
Gck	TGAGCCGGATGCAGAAGGA	GCAACATCTTTACACTGGCCT
Gpt2	GAAGGAAGTAGCCGCATCCA	AGGAAAAGCTGTAGACCGTCACA
Ldha	ATGCACCCGCCTAAGGTTCTT	TGCCTACGAGGTGATCAAGCT
ChREBP α	CGACACTCACCCACCTCTTC	CTTGTCCCGGCATAGCAAC
ChREBP β	TCTGCAGATCGCGTGGAG	TTGTTCAGCCGGATCTTGTC
Acacb	CGCTCACCAACAGTAAGGTGG	GCTTGGCAGGGAGTTCCTC
Srebp1c	GGAGCCATGGATTGCACATT	GGCCCGGGAAGTCACTGT
Fasn	GAGGTGGTGATAGCCGGTATG	GACCGCTTAGGCAACCCA
Actb	CCAGATCATGTTTGAGACCTTC	CATGAGGTAGTCTGTCAGGTCC

LDHA: 30%; GPT2: 54%, $P < 0.06$) and triglyceride content (GCK: 20%; LDHA: 13%; GPT2: 47%, $P < 0.07$) (**Fig. 2**). For changes in parameters without a stated *P*-value, $P > 0.3$.

DNL is increased in 6-week HFD-fed mice

Six-week high-fat diet-fed mice (overnutrition), as compared with 3-day high-fat diet-fed mice (control), have a significant increase in hepatic lipogenesis (42%), as well as significantly increased liver (188%) and serum (79%) TG concentrations (**Fig. 3**). This is consistent with data previously described in both mouse models and in humans, where insulin-resistant subjects have increased levels of DNL when compared to insulin-sensitive subjects (4, 6, 11, 29). Furthermore, the hepatic concentrations of many metabolites of intermediary metabolism were assessed via a GC-MS-based metabolomics approach. Critical hepatic TCA cycle intermediates, including fumarate, malate, and citrate, are significantly increased in the ON mice (ON control vs. CO control: fumarate +74.2% ± 78.4, $P < 0.05$; malate +54.0% ± 35.5, $P < 0.05$; and citrate +43.2 ± 25.6, $P < 0.001$). Interestingly, several amino acids, including leucine, isoleucine, valine, and serine, have significantly decreased hepatic concentrations in the ON mice (ON control vs. CO Control: Leu −41.7% ± 30.4, $P < 0.01$; Ile −45.0% ± 26.9, $P < 0.01$; Val −56.3% ± 22.0, $P < 0.001$; Ser −22.6 ± 22.0, $P < 0.01$). In summary, mice with chronic overnutrition, as compared with relatively insulin-sensitive short-term high-fat diet-fed mice, not only demonstrate increased DNL but also demonstrate an increase in the concentration of TCA cycle intermediates, while hepatic amino acid concentrations are decreased.

Maintaining DNL in overnourished mice requires the availability of multiple carbon sources

In 6-week high-fat fed mice, ASO treatment knocked down target genes and proteins (**Fig. 1**). The GCK ASO induced a 69% reduction in hepatic DNL, a 59% reduction in liver TGs, and a 36% decrease in serum TG, compared to the same ON mice treated with a control ASO (**Fig. 4**). Similarly, LDHA ASO treatment caused a 33% reduction in DNL and a 26% reduction in hepatic TGs. Lastly, the ON mice treated with the GPT2 ASO demonstrated a 48% decrease in hepatic DNL, a 45% reduction in liver TGs, and a 23% decrease in serum TGs. Therefore, in the setting of chronic overnutrition, where there are heightened rates of DNL, glucose, lactate, and alanine are all essential to maintaining heightened rates of hepatic lipogenesis.

Glucokinase knockdown attenuates lipogenesis to a 44% greater degree in ON mice than compared to the GPT2 ASO. In conjunction with the decreased rates of DNL observed multiple intrahepatic metabolites were decreased in the ON GCK ASO-treated mice. There is a significant decrease in hepatic alanine (57%), lactate (43%), and citrate (39%), with a trending reduction in hepatic glutamate (65%) (**Fig. 5**). There were no significant alterations in these metabolites in any of the other treatment groups (Supplemental Fig. 1).

Some effects of LDH ASO may be mediated by an altered cytosolic redox state

Potential alterations to both mitochondrial and cytosolic redox states were assessed by Beta-hydroxybutyrate (βHB) to acetoacetate (AcAc) ratio and lactate to pyruvate ratio, respectively. A slight increase in lactate: pyruvate ratio was observed in MOE control treated after 6 weeks of high-fat feeding, compared to 3-day high-fat fed mice, although this was not observed in GalNAc ASO treated mice. Furthermore, the LDHA ASO caused a significant reduction in lactate: pyruvate ratio in 6-week high-fat fed mice (**Fig. 6**). No significant differences were seen in the mitochondrial redox state as measured by βHB: AcAc ratio (Supplemental Fig. 2). Thus, an increase in reduced NADH (or NADPH) could help to account for increased DNL in fat-fed mice, and a decrease in reduced equivalents may contribute to the decrease in DNL seen in LDHA ASO treated mice.

Carbon flux into citrate is increased with chronic overnutrition and reduced with GCK ASO

In MOE ASO control mice relative carbon flux through citrate synthase (CS) ($P < 0.01$), isocitrate dehydrogenase (IDH) ($P < 0.05$), and ATP-citrate lyase (ACLY) ($P < 0.05$), as reflected by altered label distribution within TCA cycle intermediates, are all significantly increased in ON mice compared with CO mice (**Fig. 7**). In GalNAc ASO control mice similar results are observed with a significant increase in relative CS flux ($P < 0.05$), and a trending increase in both IDH ($P < 0.1$)

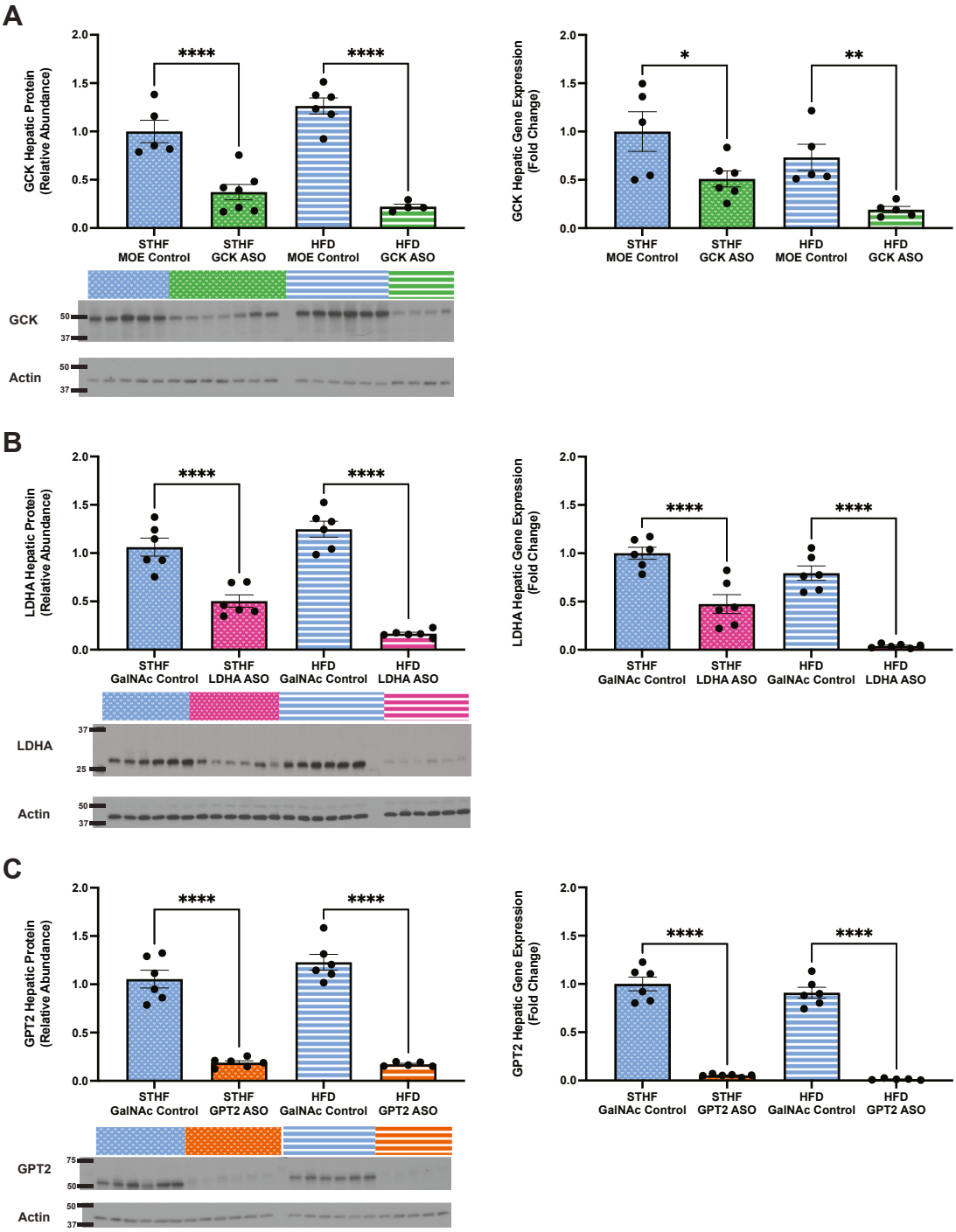

Fig. 1. Confirmation of hepatic knockdown. Hepatic protein and gene expression were analyzed in GCK (A), LDHA (B), and GPT2 (C) cohorts to confirm knockdown in gene expression and translation of ASO targets, compared to controls. Blots of target and control proteins are provided below graphs quantifying protein abundance. N = 5–6 per group. Data are represented as mean ± SEM. Statistical comparisons by ordinary one-way ANOVA, followed by a Fisher's LSD post-hoc comparison after confirmation of a significant ANOVA result. The *P*-value is denoted by a * for $P < 0.05$, ** for $P < 0.01$, *** for $P < 0.001$, and **** for $P < 0.0001$. Each dot represents a biological replicate.

and ACLY ($P < 0.2$) in ON compared with CO mice. Furthermore, in ON mice, administration of the GCK ASO significantly reduced relative IDH flux ($P < 0.05$), and trending reductions in both CS (p~0.05) and ACLY (p~0.2) flux were observed. In an internally consistent manner, relative ACLY flux changes were reflected in opposite relative changes in SDH fluxes (Supplemental Fig. 3). Consistent with the DNL measurement experiments, relative ACLY flux changes went in the same direction as changes in DNL.

If the ASOs inadvertently altered peripheral proteolysis, this could explain some of the observed changes

TABLE 2. Characterization of fed-state (2h fasted) mice, fed high fat diet with 1% dextrose water supplementation. Mouse weights at euthanasia. Data represented as mean ± SEM

Group	Measure (2-h Fasted)	STHF Control	STHF ASO	HFD Control	HFD ASO
GCK	Mouse Weight (g)	30.7 ± 1.02	27.0 ± 0.5	41.3 ± 3.9	34.1 ± 1.2
	Serum Glucose (mg/dl)	223 ± 17.6	237 ± 11.2	238 ± 4.5	241 ± 13.3
	Serum Insulin (μU/ml)	38.4 ± 3.8	42.0 ± 5.0	38.4 ± 5.1	45.8 ± 5.7
	ALT (U/L)	15.9 ± 3.5	9.0 ± 0.7	10.7 ± 2.8	6.7 ± 0.4
	AST (U/L)	58.2 ± 13.5	45.9 ± 7.0	28.3 ± 4.8	28.8 ± 2.0
LDHA	Mouse Weight (g)	25.5 ± 1.0	29.2 ± 0.4	38.4 ± 0.7	35.9 ± 1.1
	Serum Glucose (mg/dl)	246 ± 9.7	211 ± 14.5	252 ± 17.6	244 ± 9.5
	Serum Insulin (μU/ml)	43.0 ± 10.3	41.6 ± 2.6	45.7 ± 13.3	41.1 ± 7.5
	ALT (U/L)	11.2 ± 0.8	16.3 ± 5.8	9.8 ± 1.1	7.0 ± 0.2
	AST (U/L)	61.8 ± 7.9	77.8 ± 12.1	32.0 ± 4.1	22.6 ± 2.1
GPT2	Mouse Weight (g)	25.5 ± 1.0	29.7 ± 0.4	38.4 ± 0.7	37.7 ± 1.3
	Serum Glucose (mg/dl)	246 ± 9.7	230 ± 11.5	252 ± 17.6	249 ± 5.5
	Serum Insulin (μU/ml)	43.0 ± 10.3	34.3 ± 5.0	45.7 ± 13.3	36.0 ± 2.5
	ALT (U/L)	11.2 ± 0.8	36.4 ± 6.5	9.8 ± 1.1	8.2 ± 0.7
	AST (U/L)	61.8 ± 7.9	108.5 ± 21.6	32.0 ± 4.1	29.4 ± 3.2

in intrahepatic amino acid concentration and could disproportionately influence carbon flux to DNL. While this study was not designed to measure amino acid turnover, turnover is inversely proportional to enrichment of the infused isotope, so plasma m+5 enrichment was measured, and was unchanged (Supplemental Fig. 4).

Molecular lipogenic programming is decreased with GPT2 and LDHA ASOs but not GCK ASO

Both insulin and substrate can promote the transcription of lipogenic machinery through SREBP-1c and ChREBP, respectively. In CO mice, GPT2 ASO administration significantly reduced the expression of *Chrebp β* by 72% ($P < 0.05$) (**Fig. 8**). With the LDHA ASO, a similar trend was observed in the expression of *Chrebp β* (57%, $P < 0.055$), and a significant reduction was observed in both *Acacb* (44%, $P < 0.05$) and *Fasn* (46%, $P < 0.05$) in CO mice. With the GCK ASO, these effects on the molecular control of lipogenesis were not observed in CO mice. In ON mice treated with the GCK ASO, no significant changes were seen in the molecular control of hepatic lipogenesis. However, in the setting of ON, administration of either the GPT2 or LDHA ASO induced significant reductions in *Chrebp β* (GPT2: −63%, $P < 0.05$; LDHA: −69%, $P < 0.01$), *Srebp1c* (GPT2: −74%, $P < 0.05$; LDHA: −86%, $P < 0.01$), *Acacb* (GPT2: −74%, $P < 0.05$; LDHA: −90%, $P < 0.001$), and *Fasn* (GPT2: −69%, $P < 0.05$; LDHA: −83%, $P < 0.05$). Overall, the use of either the GPT2 or LDHA ASOs reduced lipogenic gene expression, while the GCK ASO did not significantly alter the molecular regulation of hepatic lipogenesis.

DISCUSSION

Increased de novo lipogenesis contributes to lipid disturbances prevalent in insulin-resistant subjects, including dyslipidemia and MASLD; however, the contributions of different lipogenic substrates to the increase in DNL seen in the setting of insulin resistance remains largely unexplored (4–6). To address these questions, ASOs targeting glucokinase, lactate dehydrogenase, and glutamic-pyruvic transaminase 2 were utilized to restrict substrate influx from specific lipogenic precursors in both relatively insulin-sensitive control mice, and 6-week high-fat diet-fed mice (chronic overnutrition). Restriction of substrate supply had markedly different effects on CO mice compared to ON mice. Only with the restriction of alanine import through GPT2 knockdown were there significantly altered lipogenesis in CO mice, while all three ASOs diminished lipogenesis in ON mice.

Glucose and fructose are major lipogenic substrates (30, 31), and these carbohydrates can drive the lipogenic transcriptional program. Insulin drives lipogenic gene expression via SREBP-1c, and carbohydrate catabolism can increase lipogenesis via activation of the transcription factor ChREBP (7, 9, 13). Even though dietary carbohydrates can drive lipogenesis, it has been posited that neither dietary glucose nor fructose, are major carbon sources for hepatic lipogenesis in healthy mice (17, 32, 33). In this study, we probed this concept further to demonstrate which substrates are the predominant lipogenic carbon sources in differentially fat-fed mice.

Restricting glucose or lactate entry into hepatocyte metabolism in CO mice only caused a slight, nonsignificant, reduction in hepatic DNL. This is consistent with prior literature suggesting diminished importance of glucose carbon in lipogenesis (17, 32). However, the GPT2 ASO did cause a robust reduction in both DNL and hepatic triglyceride content—albeit still insignificant. Together, these findings support the idea that amino acids, and not carbohydrates, provide the most significant amount of lipogenic carbon in healthy mice.

Congruent with previous findings in both insulin-resistant rodent models and insulin-resistant humans, hepatic DNL is elevated in our mouse model of high-fat-fed overnutrition (4, 5). In humans with hepatic steatosis, insulin resistance correlates

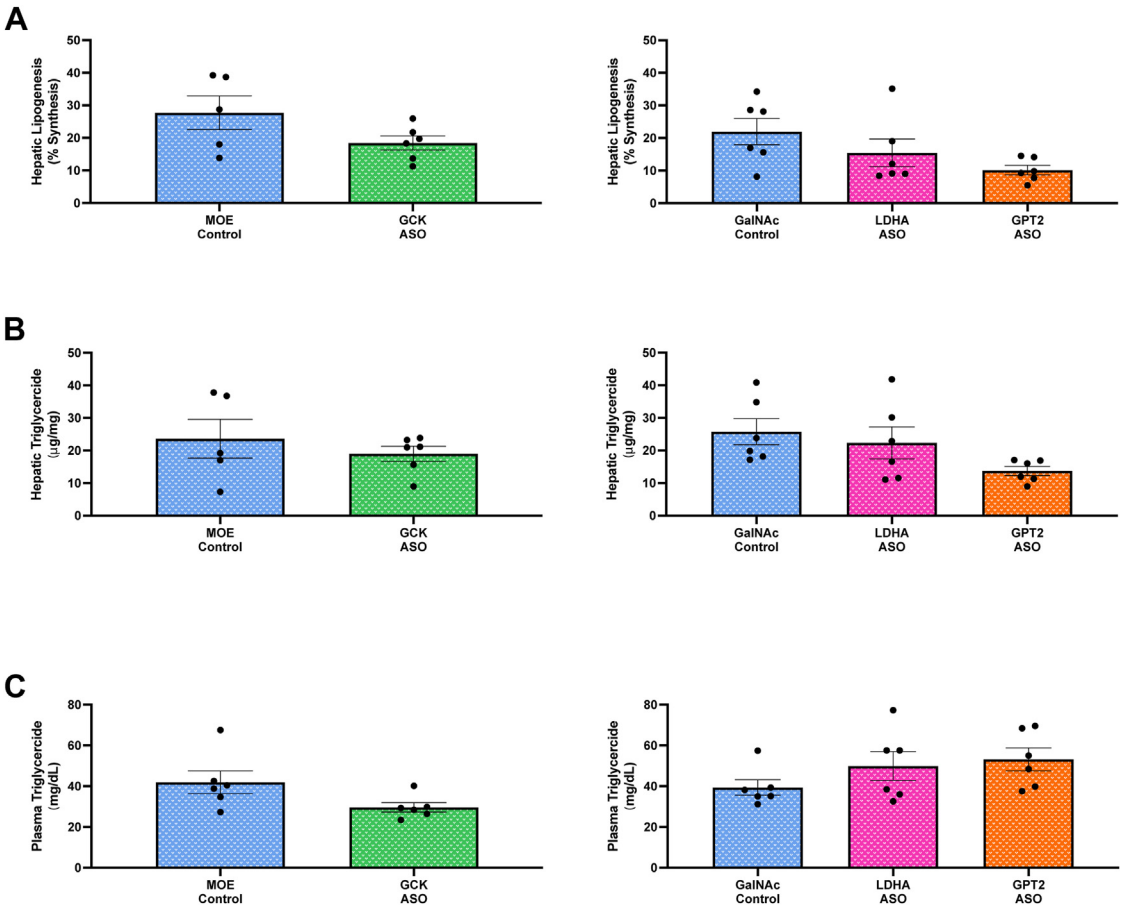

Fig. 2. Hepatic lipogenesis in short-term fat-fed ASO-treated mice. Hepatic DNL (A), hepatic triglyceride content (B), and serum triglyceride (C) were measured in GCK ASO, LDHA ASO, and GPT2 ASO groups. N = 5–6 mice per group. Data are represented as mean ± SEM. Statistical comparisons for GCK ASO by Student's two-tailed *t* test. Statistical comparisons for LDHA and GPT2 ASOs by an ordinary one-way ANOVA, followed by a Dunnett's multiple comparisons test. Each dot represents a biological replicate.

with an increase in circulating concentrations of precursors of triglyceride biosynthesis (20), suggesting carbon flux to the liver is a critical link between whole-body insulin resistance and hepatic steatosis. In this study, the ON mice, compared with CO mice, have significantly increased rates of lipogenesis. This increase in DNL is supported by both an increase in lipogenic gene expression and an increase in carbon flux to citrate. Furthermore, restricting entry into the pyruvate pool in ON mice from any carbon source—lactate, alanine, or especially glucose—resulted in a significant reduction of hepatic DNL. Interestingly, the regulation of this decrease in lipogenesis appears different between the GCK ASO group and both the LDHA or GPT2 cohorts. The observed increase in carbon flux to citrate in ON mice is significantly diminished with GCK ASO administration, but not significantly altered with LDHA or GPT2 ASO administration. Whether these insignificant changes to carbon flux in either LDHA or GPT2 groups is due to unmodified carbon flux, or whether there are differences below our ability to detect, remains an open question.

In contrast, the elevated lipogenic gene expression seen in ON mice is abrogated by the LDHA and GPT2 ASOs but is not altered by treatment with the GCK ASO. A priori, we hypothesized that if any of the tested ASOs would alter lipogenic gene expression, GCK ASO would do so most prominently. Beyond its role as a carbon source, carbohydrates can activate the transcription of lipogenic machinery via ChREBP. It is thought that glucose-6-phosphate (G6P), or another intermediate metabolite of glucose catabolism, promotes ChREBP activation (15, 34, 35). These results suggest that the critical ChREBP-activating metabolite is further downstream from glucose than glucose-6-phosphate, such that we see an impact from partial knockdown of LDHA and GPT2, but not GCK. While it is difficult to explain the lack of an impact on ChREBP expression in mice with reduced glucokinase, the reduced lipogenic transcription factor pattern seen in the LDHA ASO and GPT2 ASO could potentially be explained by alterations in substrate-responsive AMPK, cholesterol-regulated LXR, or redox-regulated Sirt6 (36–40). Further studies are required to interrogate these mechanisms.

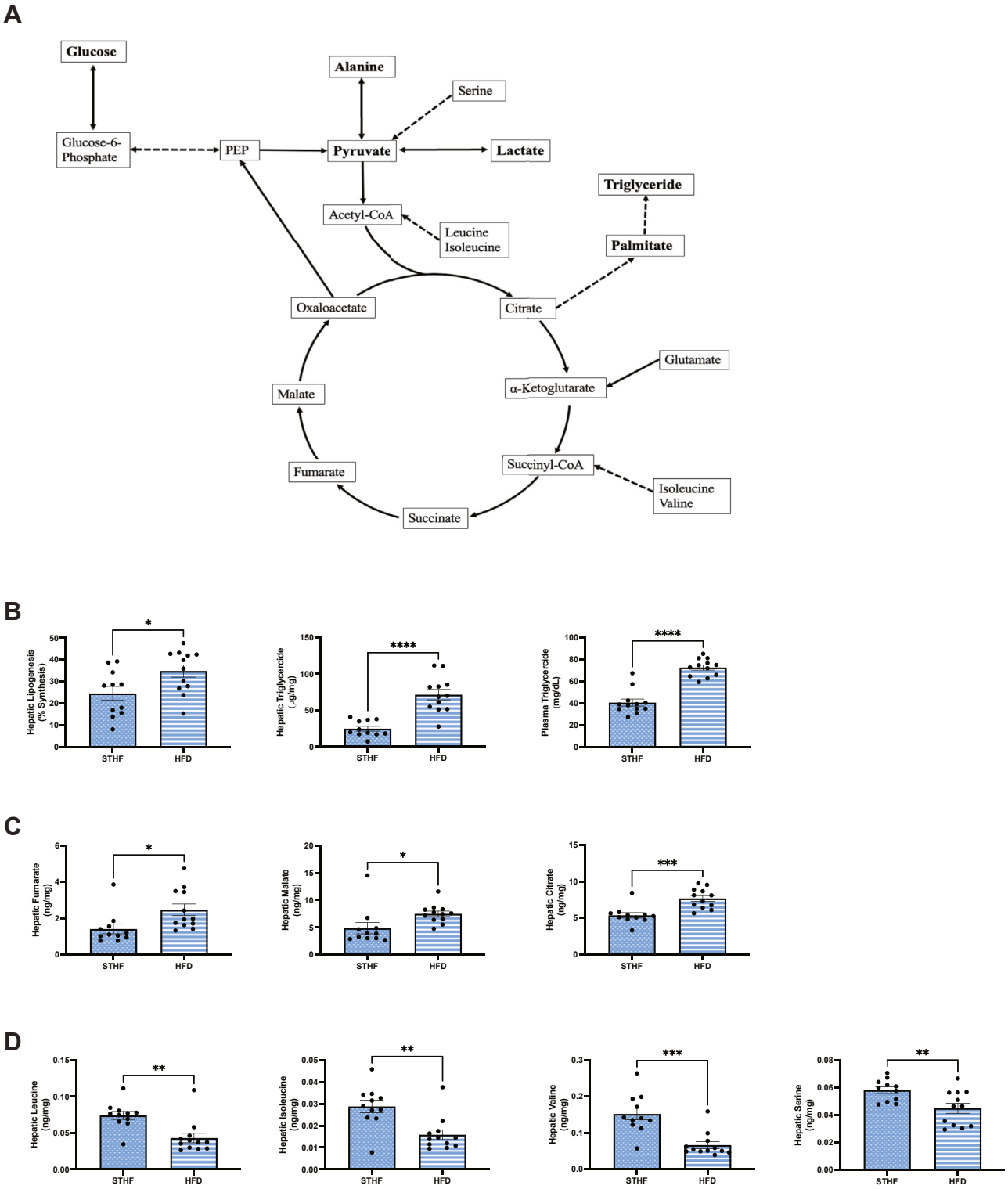

Fig. 3. Hepatic lipogenesis is increased in mice with chronic overnutrition. A simple schematic overview (A) of hepatic production of mitochondrial pyruvate and de novo lipid synthesis is provided. Hepatic DNL (B), hepatic TCA cycle intermediate concentrations (C), and hepatic amino acid concentrations (D) were measured in both short-term high-fat-fed (control) and 6-week high-fat-fed (chronic overnutrition) groups. N = 11–12 mice per group. Data are represented as mean ± SEM; statistical comparisons by Student's two-tailed *t* test. The *P*-value is denoted by a * for $P < 0.05$, ** for $P < 0.01$, *** for $P < 0.001$, and **** for $P < 0.0001$. Each dot represents a biological replicate.

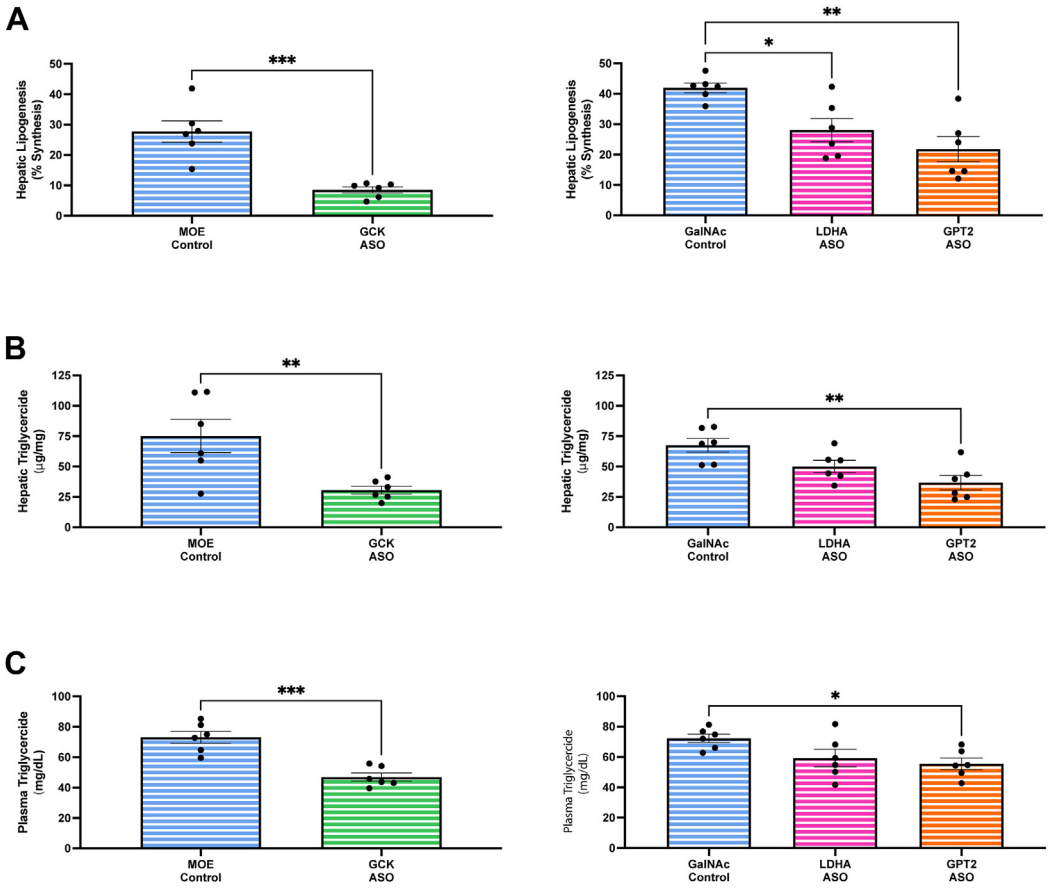

Fig. 4. Hepatic lipogenesis in ASO-treated mice with chronic overnutrition. Hepatic DNL (A), hepatic triglyceride content (B), and serum triglyceride (C) were measured in GCK, LDHA, and GPT2 groups to assess hepatic lipogenesis in 6-weeks high-fat diet-fed (chronic overnutrition) C57BL6/J mice. N = 6 mice per group. Data are represented as mean ± SEM. Statistical comparisons for GCK ASO by Student's two-tailed *t* test. Statistical comparisons for LDHA and GPT2 ASOs by an ordinary one-way ANOVA, followed by a Dunnett's multiple comparisons test. The *P*-value is denoted by a * for $P < 0.05$, ** for $P < 0.01$, *** for $P < 0.001$, and **** for $P < 0.0001$. Each dot represents a biological replicate.

Together these data suggest a greater role for altered lipogenic carbon flux in the attenuation of DNL due to GCK ASO administration, whereas molecular regulation of lipogenic program has a greater role in the attenuation of DNL due to LDHA and GPT2 ASO administration. Furthermore, the reversal of the pro-lipogenic redox state of ON mice by the LDHA ASO may also help to explain the effect of this ASO. While the mechanism of action may be different between ASOs, reducing carbon from glucose, lactate, or alanine all decrease the heightened rates of DNL observed in ON mice. Notably, the alterations to carbon flux are not an artifactual effect of the ASOs on rates of peripheral proteolysis.

As noted above, it has been posited that glucose is not a major carbon source for hepatic lipogenesis (17). Our data is consistent with this observation, as restricting glucose entry into glycolysis did not limit DNL in the CO mice. Of note, prior studies interrogating the reliance on glucose to support hepatic lipogenesis have been performed in insulin-sensitive mice (17, 32), leaving open the critical question of whether glucose is important for the stimulation of DNL seen in insulin-resistant animals. Interestingly, data from the present study supports the idea that hepatic glucose entry is essential to maintaining hepatic DNL in the setting of overnutrition. Extrapolating from studies of the role of glucose in insulin-sensitive mice to the insulin-resistant condition may have created discordant or even incorrect conclusions in the past. The results presented here are consistent with a significantly different role for glucose in DNL in CO versus ON mice. While restricting hepatocyte glucose entry with the glucokinase ASO in CO mice had minimal effect on DNL, restricting glucose to ON livers dramatically disrupted DNL. Glycolysis appears replaceable for maintenance of DNL in the CO mouse, while it is indispensable in the ON mouse.

Not only does glucose appear to play a role in DNL in ON mice that it does not in relatively insulin-sensitive mice, but hepatic glucose input into DNL in ON mice is particularly important. The GPT2 ASO, which was the only ASO to attenuate lipogenesis (by a nearly-significant trend) in CO mice, decreased DNL

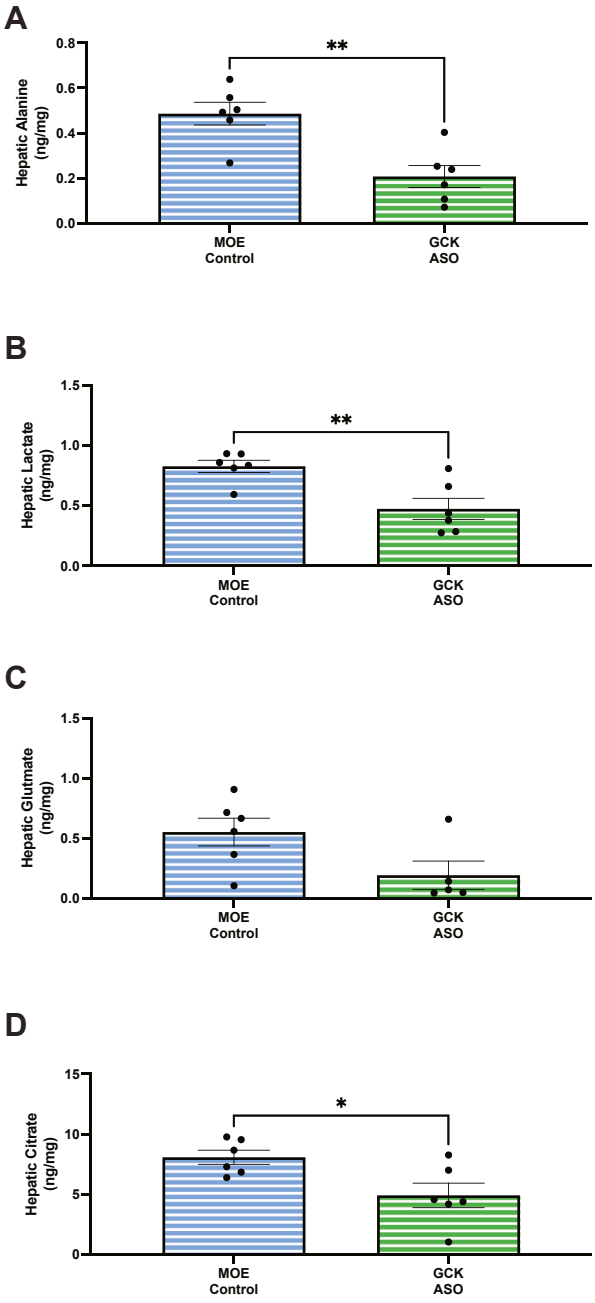

Fig. 5. Hepatic metabolite concentrations GCK ASO-treated mice with chronic overnutrition. Hepatic concentrations alanine (A), lactate (B), glutamate (C), and citrate (D) were assessed in mice compared to control mice after 6 weeks of a high-fat diet (chronic overnutrition). N = 5–6 mice per group. Data are represented as mean ± SEM; statistical comparisons by Student's two-tailed *t* test. The *P*-value is denoted by a * for $P < 0.05$, ** for $P < 0.01$, *** for $P < 0.001$, and **** for $P < 0.0001$. Each dot represents a biological replicate.

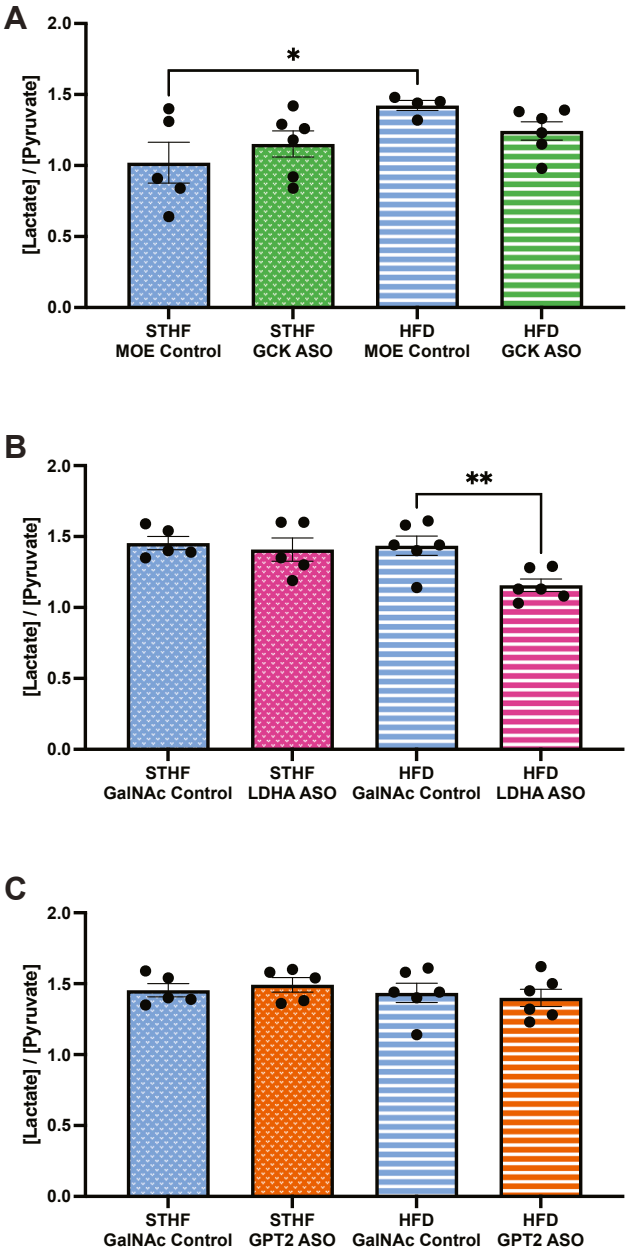

Fig. 6. Cytosolic redox state. Hepatic lactate to pyruvate ratio was quantified for a measure of cytosolic redox state in the GCK (A), LDHA (B), and GPT2 (C) groups. N = 5–6 per group. Data are represented as mean ± SEM. Statistical comparisons by ordinary one-way ANOVA, followed by a Fisher's LSD post-hoc comparison after confirmation of a significant ANOVA result. The *P*-value is denoted by a * for $P < 0.05$, ** for $P < 0.01$, *** for $P < 0.001$, and **** for $P < 0.0001$. Each dot represents a biological replicate.

by 48% in ON mice. In contrast, while the GCK ASO did not have a significant impact on DNL in CO mice, it markedly knocked down DNL in ON mice (by 69%). The ON GCK ASO-treated mice also demonstrated significant reductions in hepatic concentrations of many alternative substrates (eg alanine and lactate), reflecting the impact of reduced glucose metabolism on other carbon sources for DNL. In the setting of overnutrition, carbohydrate use by the hepatocyte appears to be essential for maintaining elevated rates of hepatic lipogenesis. This study demonstrates that carbohydrate, and lipogenic substrate in general, can drive DNL in addition to the well-described effects of carbohydrate on the transcription of lipogenic enzymes.

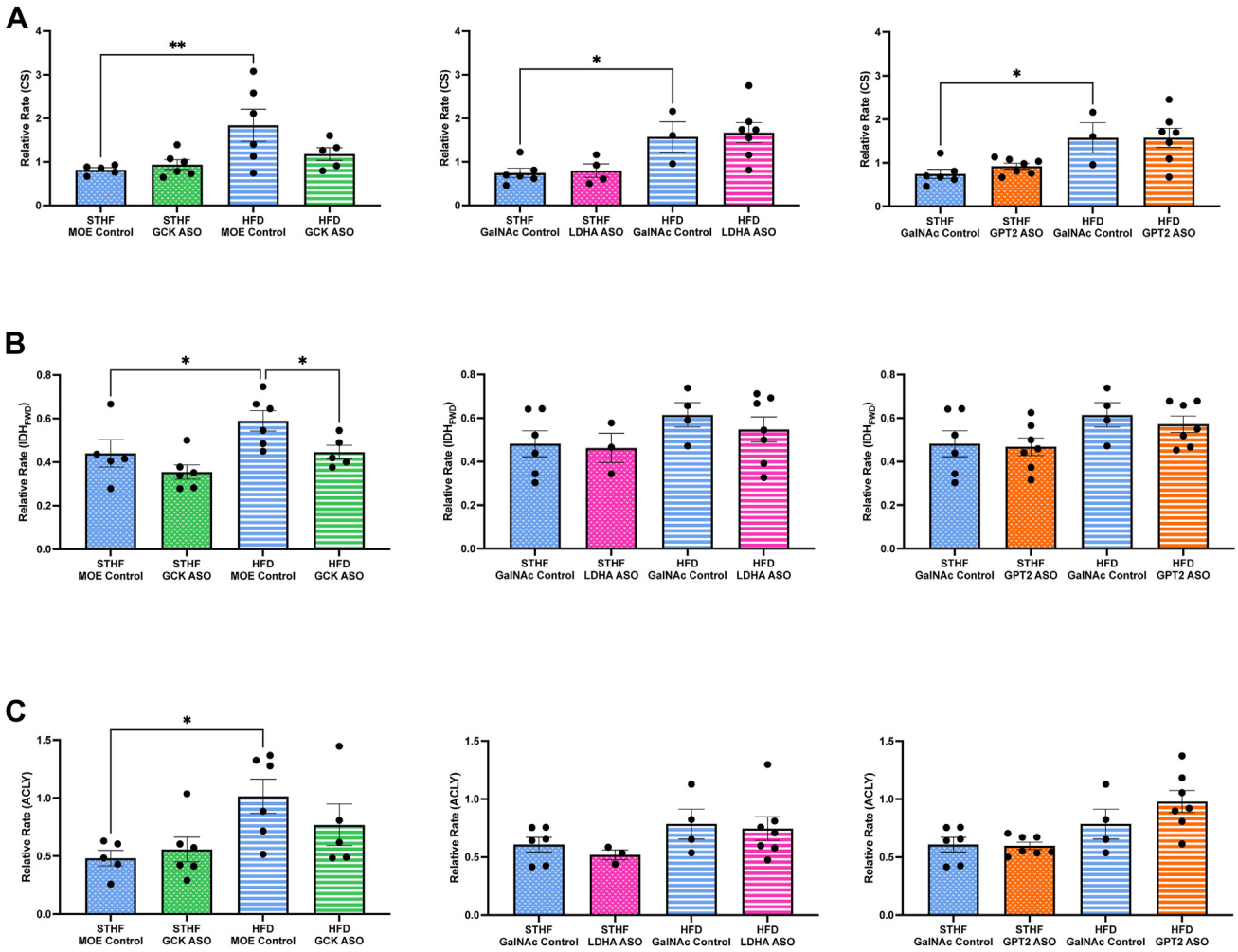

Fig. 7. Relative carbon 13 label into citrate. Uniformly labeled glutamine was infused in ASO-treated mice to determine differences in carbon label distribution into citrate synthase (A), isocitrate dehydrogenase (B), and ATP-citrate lyase (C) induced by diet and ASO treatment. N = 5–6 per group. Data are represented as mean ± SEM. Statistical comparisons by ordinary one-way ANOVA, followed by a Fisher's LSD post-hoc comparison after confirmation of a significant ANOVA result. The *P*-value is denoted by a * for $P < 0.05$, ** for $P < 0.01$, *** for $P < 0.001$, and **** for $P < 0.0001$. Each dot represents a biological replicate.

This study has some limitations that should be acknowledged. For this investigation, we chose to evaluate only three ASOs, even though many enzymes are critical to substrate availability for DNL. However, in vivo lipogenic flux measurements are quite variable, so performing a screening study testing all anaplerotic and glycolytic enzymes would be impractical in combination with stable isotope measurements of DNL. However, in this study, using only three ASO targets, we were able to clearly demonstrate the important effect of individual lipogenic substrates on DNL. A second concern is regarding the bidirectional nature of some metabolic enzymes. Both LDHA and GPT2 can regulate flux both into and away from mitochondrial pyruvate. This enzymatic bidirectionality has the potential to confound some of the interpretation of the results from these experiments.

Furthermore, as with any dietary intervention, the composition of the diet and the substrates provided can influence hepatic metabolism and carbon flux. While a 60% high-fat diet does not mimic the nutrient composition of American high-calorie diets (~36% calories from fat, CDC National Center for Health Statistics), and laboratory rodents don't mimic the genetic variation in human patients, results from HFD-fed rodents studies have been remarkably translatable to human insulin resistance. Bioactive lipid paradigms for insulin resistance, such as the diacylglycerol and ceramide models of insulin resistance, are consistently reproducible in human studies (41, 42).

For this study, we used 3-day high-fat fed mice as a control cohort compared to the 6-week high-fat fed mice. This allows the mice to be matched in terms of substrate, which is critical for direct comparisons of DNL between the groups. We have previously shown that this comparison is reasonable when considering the important parameter of insulin resistance: a short-term high-fat diet/dextrose water-fed model is relatively insulin sensitive as compared with longer-term fat-fed mice (23). However, we cannot rule out that a

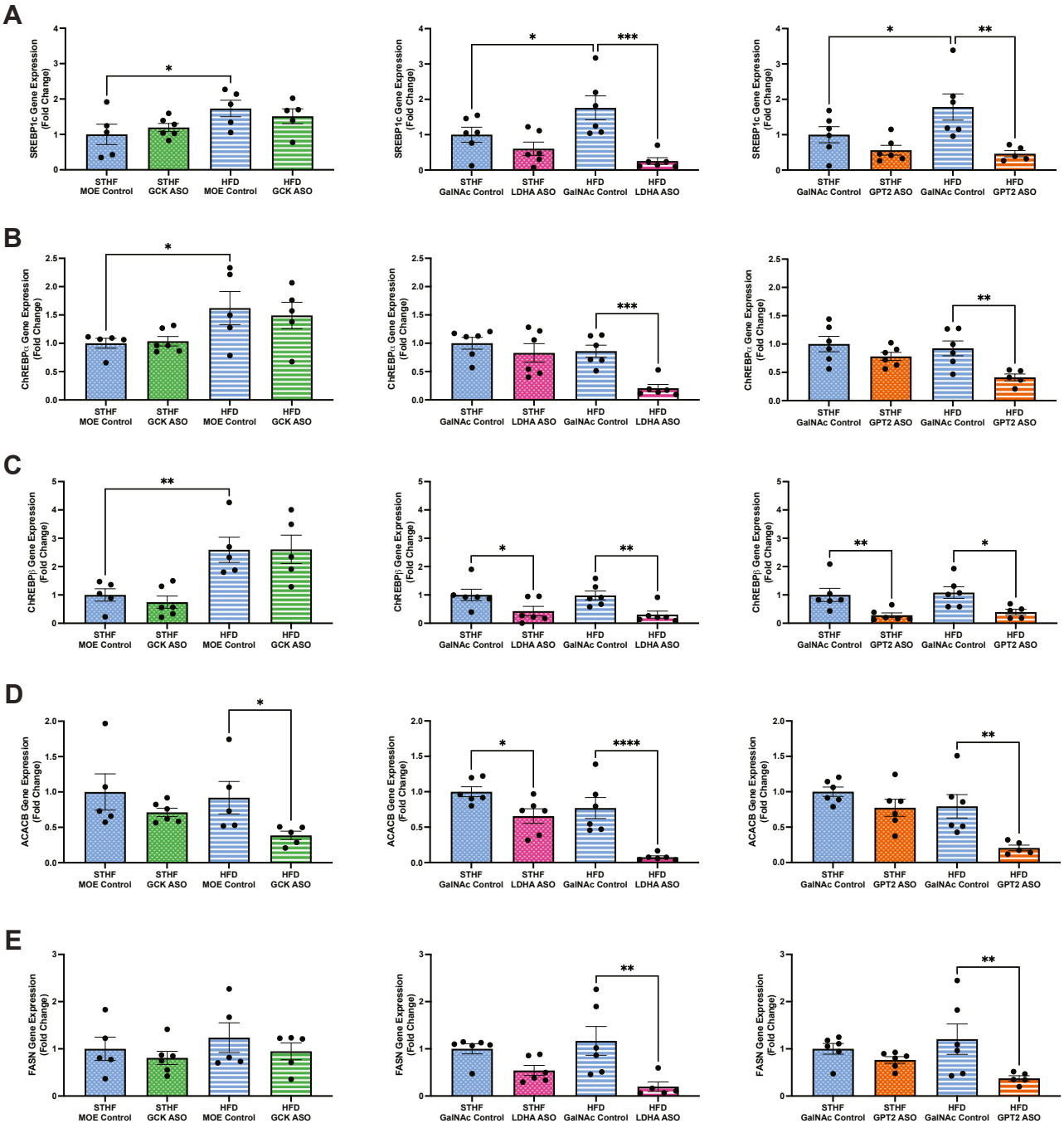

Fig. 8. DNL-associated gene expression. Hepatic expression of *Srebp1c* (A), *Chrebp α* (B), *Chrebp β* (C), *Acacb* (D), and *Fasn* (E) were measured via qPCR in both short-term high-fat-fed (control) or 6-week high-fat diet fed (overnutrition) mice. N = 5–6 mice per group. Data are represented as mean ± SEM. Statistical comparisons by ordinary one-way ANOVA, followed by a Fisher's LSD post-hoc comparison after confirmation of a significant ANOVA result. The *P*-value is denoted by a * for $P < 0.05$, ** for $P < 0.01$, *** for $P < 0.001$, and **** for $P < 0.0001$. Each dot represents a biological replicate.

more insulin-sensitive model might route its carbon fluxes to DNL in a meaningfully different way—for example, increased beta-oxidation with a high-fat diet will alter the mitochondrial acyl CoA profile, which directly impacts multiple TCA cycle-adjacent fluxes.

Furthermore, when measuring lipogenesis on a high-fat diet, a source of lipogenic substrate is required to get robust, interpretable results. The decision to use carbohydrates in the drinking water certainly amplified the importance of glucokinase in this study; however, the addition of sugar to the diet was necessary to elevate levels of lipogenesis to levels where differences could be detected between cohorts. This dietary condition also better reflected a 'Western diet'—high in both fat and sugar. Furthermore, in the overnourished cohort, the knockdown of any gene involved in the

entry of carbon into pyruvate led to a decrease in DNL. Thus, if we had chosen another lipogenic carbon source in this study (eg alanine), we would expect a similar result (although a result that may amplify the importance of the other chosen lipogenic substrate). While one might propose to study a battery of diets to better understand the discrete roles of each lipogenic substrate, our study design, using a single diet, allowed for a more straightforward comparison between experimental groups.

Finally, in this study, we utilized a uniformly labeled glutamine tracer to assess relative carbon flux, as well as measure rates of peripheral proteolysis. In future studies, alternative tracer methods, such as developing a new method to follow amino acid carbons into fatty acids, could be employed to better evaluate the fate of specific carbon sources into fatty acids. Still, the data presented in this study uncovers how substrate flux from different precursors is incorporated into fatty acids.

In conclusion, DNL in mice is dependent on all substrate fluxes to the liver. However, while some flexibility exists in the more insulin-sensitive condition, in the overnourished whole-body insulin-resistant condition the reliance of hepatic lipogenesis on specific substrates is dramatically altered and the elevated rates of hepatic DNL are markedly attenuated when entry of any lipogenic metabolite is restricted. These findings may inform the development of novel therapies and underscore the importance of the interplay between peripheral substrate metabolism (uptake, production, and oxidation) and the liver in the regulation of hepatic lipogenesis, impacting on both the development of and prevention of fatty liver disease and dyslipidemia in the metabolic syndrome.

Data availability

All data described in the manuscript is provided either within the document or in the supplemental material.

Supplemental data

This article contains supplemental data.

Acknowledgments

We would like to thank the lab of Gerald I. Shulman, including Brandon Hubbard and John Stack, as well as Ali Nasiri and the Yale Mouse Metabolic Phenotyping Center In Vivo Physiology Core (funded through the NIDDK Mouse Metabolic Phenotyping Centers [MMPC-Live, RRID:SCR_008997, www.mmpc.org] under the MMPC-Live Program) for assistance with the design and execution of the tracer infusion study. We thank Dr Richard G. Kibbey and the Yale Chemical Metabolism Core (Yale School of Medicine) for the mass spectrometry-based isotopomer analysis and helpful discussion regarding the results. We would also like the thank Dr Varman T. Samuel for useful discussion and manuscript review.

Author contributions

J. W. S., C. R. G., and D. F. V. writing–review & editing; J. W. S. and D. F. V. writing–original draft; J. W. S. visualization; J. W. S., S. S., S. F. M., and C. R. G. methodology; J. W. S., S. S., and M. G. investigation; J. W. S., S. S., and C. R. G. formal analysis; J. W. S. and D. F. V. conceptualization; S. F. M. resources; C. R. G. and D. F. V. supervision; D. F. V. funding acquisition.

Author ORCIDs

Jordan W. Strober https://orcid.org/0000-0001-8274-3956
Susan F. Murray https://orcid.org/0000-0002-7302-624X
Manuel González Rodríguez https://orcid.org/0000-0002-1227-2391
Carlos Rodriguez-navas Gonzalez https://orcid.org/0000-0002-8499-5513
Daniel F. Vatner https://orcid.org/0000-0003-2073-0273

Funding and additional information

This study was supported by grants from the National Institutes of Health (R01 DK124272 (D. F. V.), T32 DK007058 (J. W. S.), the Yale Diabetes Research Center P30 D3K04575, and the Yale MMPC U2C DK134901).

Conflict of interests

The authors declare the following financial interests/personal relationships which may be considered as potential competing interests: SFM reports being an employee and shareholder of Ionis Pharmaceuticals. The other authors declare that there is no competing interest associated with their contribution to this manuscript.

Abbreviations

ACACB, Acetyl-CoA Carboxyalse 2; ALT, Alanine Transaminase; AMPK, AMP-activated protein kinase; ASCVD, Atherosclerotic Cardiovascular Disease; ASO, Antisense Oligonucleotides; AST, Aspartate Aminotransferase; ChREBP, Carbohydrate Response Element Binding Protein; CO, Control; DNL, De Novo Lipogenesis; FASN, Fatty Acid Synthase; G6P, Glucose-6-Phosphate; GalNAc, N-Acetylgalactosamine; GCK, Glucokinase; GPT2, Glutamic-Pyruvic Transaminase 2; HFD, High-Fat Diet; Ile, Isoleucine; LDHA, Lactate Dehydrogenase A; Leu, Leucine; LXR, Liver X Receptor; MASLD, Metabolic dysfunction-Associated Steatotic Liver Disease; MLXIPL, MLX Interacting Protein Like; MOE, 2′-O-methoxyethyl; ON, Chronic Overnutritions; Ser, Serine; Sirt6, Sirtuin 6; TG, Triglyceride; Val, Valine.

Manuscript received March 16, 2024, and in revised form May 29, 2025. Published, JLR Papers in Press, June 9, 2025, https://doi.org/10.1016/j.jlr.2025.100838

REFERENCES

1. Committee, A.D.A.P.P.. (2021) Cardiovascular disease and risk management: standards of medical Care in diabetes—2022. *Diabetes Care.* **45 (Supplement_1)**, S144–S174. *10*
2. European Association for the Study of the, L., D. European Association for the Study of, and O. European Association for the Study of, European Association for the Study of Diabetes EASD, European Association for the Study of Obesity EASO. (2016) EASL–EASD–EASO Clinical Practice Guidelines for the management of non-alcoholic fatty liver disease. *Diabetologia.* **59**, 1121–1140

3. Younossi, Z. M., Koenig, A. B., Abdelatif, D., Fazel, Y., Henry, L., and Wymer, M. (2016) Global epidemiology of nonalcoholic fatty liver disease—meta-analytic assessment of prevalence, incidence, and outcomes. *Hepatology.* **64**, 73–84
4. Lambert, J. E., Ramos-Roman, M. A., Browning, J. D., and Parks, E. J. (2014) Increased de novo lipogenesis is a distinct characteristic of individuals with nonalcoholic fatty liver disease. *Gastroenterology.* **146**, 726–735
5. Hellerstein, M. K., Schwarz, J. M., and Neese, R. A. (1996) Regulation of hepatic de novo lipogenesis in humans. *Annu. Rev. Nutr.* **16**, 523–557
6. Donnelly, K. L., Smith, C. I., Schwarzenberg, S. J., Jessurun, J., Boldt, M. D., and Parks, E. J. (2005) Sources of fatty acids stored in liver and secreted via lipoproteins in patients with nonalcoholic fatty liver disease. *J. Clin. Invest.* **115**, 1343–1351
7. Topping, D. L., and Mayes, P. A. (1982) Insulin and non-esterified fatty acids. Acute regulators of lipogenesis in perfused rat liver. *Biochem. J.* **204**, 433–439
8. Tian, J., Goldstein, J. L., and Brown, M. S. (2016) Insulin induction of SREBP-1c in rodent liver requires LXRα-C/EBPβ complex. *Proc. Natl. Acad. Sci. U. S. A.* **113**, 8182–8187
9. Brown, M. S., and Goldstein, J. L. (1997) The SREBP pathway: regulation of cholesterol metabolism by proteolysis of a membrane-bound transcription factor. *Cell.* **89**, 331–340
10. Vatner, D. F., Majumdar, S. K., Kumashiro, N., Petersen, M. C., Rahimi, Y., Gattu, A. K., *et al.* (2015) Insulin-independent regulation of hepatic triglyceride synthesis by fatty acids. *Proc. Natl. Acad. Sci. U. S. A.* **112**, 1143–1148
11. Ter Horst, K. W., Vatner, D. F., Zhang, D., Cline, G. W., Ackermans, M. T., Nederveen, A. J., *et al.* (2021) Hepatic insulin resistance is not pathway selective in humans with nonalcoholic fatty liver disease. *Diabetes. Care.* **44**, 489–498
12. Otero, Y. F., Stafford, J. M., and McGuinness, O. P. (2014) Pathway-selective insulin resistance and metabolic disease: the importance of nutrient flux. *J. Biol. Chem.* **289**, 20462–20469
13. Yamashita, H., Takenoshita, M., Sakurai, M., Bruick, R. K., Henzel, W. J., Shillinglaw, W., *et al.* (2001) A glucose-responsive transcription factor that regulates carbohydrate metabolism in the liver. *Proc. Natl. Acad. Sci. U. S. A.* **98**, 9116–9121
14. Zhang, D., Tong, X., VanDommelen, K., Gupta, N., Stamper, K., Brady, G. F., *et al.* (2017) Lipogenic transcription factor ChREBP mediates fructose-induced metabolic adaptations to prevent hepatotoxicity. *J. Clin. Invest.* **127**, 2855–2867
15. Gong, Y., Lu, Q., Xi, L., Liu, Y., Yang, B., Su, J., *et al.* (2023) F6P/G6P-mediated ChREBP activation promotes the insulin resistance-driven hepatic lipid deposition in zebrafish. *J. Nutr. Biochem.* **122**, 109452
16. Rabøl, R., Petersen, K. F., Dufour, S., Flannery, C., and Shulman, G. I. (2011) Reversal of muscle insulin resistance with exercise reduces postprandial hepatic de novo lipogenesis in insulin resistant individuals. *Proc. Natl. Acad. Sci. U. S. A.* **108**, 13705–13709
17. Zhang, Z., TeSlaa, T., Xu, X., Zeng, X., Yang, L., Xing, G., *et al.* (2021) Serine catabolism generates liver NADPH and supports hepatic lipogenesis. *Nat. Metab.* **3**, 1608–1620
18. Yiew, N. K. H., Deja, S., Ferguson, D., Cho, K., Jarasvaraparn, C., Jacome-Sosa, M., *et al.* (2023) *Effects of hepatic mitochondrial pyruvate carrier deficiency on de novo lipogenesis and gluconeogenesis in mice. iScience.* **26**, 108196
19. Felig, P., Marliss, E., and Cahill, G. F. (1969) Plasma amino acid levels and insulin secretion in obesity. *New Engl. J. Med.* **281**, 811–816
20. Luukkonen, P. K., Qadri, S., Ahlholm, N., Porthan, K., Männistö, V., Sammalkorpi, H., *et al.* (2022) Distinct contributions of metabolic dysfunction and genetic risk factors in the pathogenesis of non-alcoholic fatty liver disease. *J. Hepatol.* **76**, 526–535
21. Turner, N., Kowalski, G. M., Leslie, S. J., Risis, S., Yang, C., Lee-Young, R. S., *et al.* (2013) Distinct patterns of tissue-specific lipid accumulation during the induction of insulin resistance in mice by high-fat feeding. *Diabetologia.* **56**, 1638–1648
22. Petersen, M. C., Madiraju, A. K., Gassaway, B. M., Marcel, M., Nasiri, A. R., Butrico, G., *et al.* (2016) Insulin receptor Thr1160 phosphorylation mediates lipid-induced hepatic insulin resistance. *J. Clin. Invest.* **126**, 4361–4371
23. Goedeke, L., Strober, J. W., Suh, R., Paolella, L. M., Li, X., Rogers, J. C., *et al.* (2024) High-fat-diet-induced hepatic insulin resistance per se attenuates murine de novo lipogenesis. *iScience.* **27**, 111175
24. Diraison, F., Pachiaudi, C., and Beylot, M. (1996) In vivo measurement of plasma cholesterol and fatty acid synthesis with deuterated water: determination of the average number of deuterium atoms incorporated. *Metabolism.* **45**, 817–821
25. Lee, W. N., Bassilian, S., Ajie, H. O., Schoeller, D. A., Edmond, J., Bergner, E. A., *et al.* (1994) In vivo measurement of fatty acids and cholesterol synthesis using D2O and mass isotopomer analysis. *Am. J. Physiol.* **266 (5 Pt 1)**, E699–E708
26. Wadke, M., Brunengraber, H., Lowenstein, J. M., Dolhun, J. J., and Arsenault, G. P. (1973) Fatty acid synthesis by liver perfused with deuterated and tritiated water. *Biochemistry.* **12**, 2619–2624
27. Alves, T. C., Pongratz, R. L., Zhao, X., Yarborough, O., Sereda, S., Shirihai, O., *et al.* (2015) Integrated, step-wise, mass-isotopomeric flux analysis of the TCA cycle. *Cell. Metab.* **22**, 936–947
28. Marin-Valencia, I., Good, L. B., Ma, Q., Duarte, J., Bottiglieri, T., Sinton, C. M., *et al.* (2012) Glut1 deficiency (G1D): epilepsy and metabolic dysfunction in a mouse model of the most common human phenotype. *Neurobiol. Dis.* **48**, 92–101
29. Petersen, K. F., Dufour, S., Savage, D. B., Bilz, S., Solomon, G., Yonemitsu, S., *et al.* (2007) The role of skeletal muscle insulin resistance in the pathogenesis of the metabolic syndrome. *Proc. Natl. Acad. Sci. U. S. A.* **104**, 12587–12594
30. Sanders, F. W. B., and Griffin, J. L. (2016) De novo lipogenesis in the liver in health and disease: more than just a shunting yard for glucose. *Biol. Rev.* **91**, 452–468
31. Softic, S., Cohen, D. E., and Kahn, C. R. (2016) Role of dietary fructose and hepatic de novo lipogenesis in fatty liver disease. *Dig. Dis. Sci.* **61**, 1282–1293
32. Baker, N., Learn, D. B., and Bruckdorfer, K. R. (1978) Re-evaluation of lipogenesis from dietary glucose carbon in liver and carcass of mice. *J. Lipid Res.* **19**, 879–893
33. Sun, S. Z., and Empie, M. W. (2012) Fructose metabolism in humans-what isotopic tracer studies tell us. *Nutr. Metab.* **9**, 89–103
34. Dentin, R., Tomas-Cobos, L., Foufelle, F., Leopold, J., Girard, J., Postic, C., and Ferré, P. (2012) Glucose 6-phosphate, rather than xylulose 5-phosphate, is required for the activation of ChREBP in response to glucose in the liver. *J. Hepatol.* **56**, 199–209
35. Xu, X., So, J. S., Park, J. G., and Lee, A. H. (2013) Transcriptional control of hepatic lipid metabolism by SREBP and ChREBP. *Semin. Liver. Dis.* **33**, 301–311
36. Kawaguchi, T., Osatomi, K., Yamashita, H., Kabashima, T., and Uyeda, K. (2002) Mechanism for fatty acid "sparing" effect on glucose-induced transcription: regulation of carbohydrate-responsive element-binding protein by amp-activated protein kinase. *J. Biol. Chem.* **277**, 3829–3835
37. Liangpunsakul, S., Ross, R. A., and Crabb, D. W. (2013) Activation of carbohydrate response element-binding protein by ethanol. *J. Investig. Med.* **61**, 270–277
38. Foretz, M., Even, P. C., and Viollet, B. (2018) AMPK activation reduces hepatic lipid content by increasing fat oxidation in vivo. *Int. J. Mol. Sci.* **19**, 2826
39. Cha, J-Y., and Repa, J. J. (2007) The liver X receptor (LXR) and hepatic lipogenesis: the carbohydrate-response element-binding protein IS a target gene of LXR. *J. Biol. Chem.* **282**, 743–751
40. Zhu, C., Huang, M., Kim, H. G., Chowdhury, K., Gao, J., Liu, S., *et al.* (2021) SIRT6 controls hepatic lipogenesis by suppressing LXR, ChREBP, and SREBP1. *Biochim. Biophys. Acta. Mol. Basis. Dis.* **1867**, 166249
41. Ter Horst, K. W., Gilijamse, P. W., Versteeg, R. I., Ackermans, M. T., Nederveen, A. J., la Fleur, S. E., *et al.* (2017) Hepatic diacylglycerol-associated protein kinase cε translocation links hepatic steatosis to hepatic insulin resistance in humans. *Cell. Rep.* **19**, 1997–2004
42. Petersen, M. C., Yoshino, M., Smith, G. I., Gaspar, R. C., Kahn, M., Samovski, D., *et al.* (2024) Effect of weight loss on skeletal muscle bioactive lipids in people with obesity and Type 2 Diabetes. *Diabetes.* **73**, 2055–2064